JOC The Journal of Organic Chemistry

ARTICLE

pubs.acs.org/joc

Kinetic Study of Proton-Transfer Reactions of Phenylnitromethanes. Implication for the Origin of Nitroalkane Anomaly

Kenichi Ando, Yu Shimazu, Natsuko Seki, and Hiroshi Yamataka*

Department of Chemistry and the Research Center for Smart Molecules, Rikkyo University, Nishi-Ikebukuro, Toshima-ku 171-8501 Tokyo, Japan

Supporting Information

ABSTRACT: Measurements of rate constants and substituent effects for three important elementary steps of proton-transfer reactions of phenylnitromethane were reported. The Hammett ρ values for the deprotonation of $ArCH_2NO_2$ with OH^-, protonation of $ArCH{=}NO_2^-$ with H_2O, and protonation of $ArCH{=}NO_2^-$ with HCl were determined in aqueous MeOH at 25 °C. Comparison of these experimentally observed ρ values with those calculated at B3LYP/6-31G* revealed that *aci*-nitro species ($ArCH{=}NO_2H$), which is formed on the O-protonation of $ArCH{=}NO_2^-$, does not lie on the main route of the proton-transfer reaction. Analysis of the Brønsted plot implies that the proton-transfer reaction of most $XC_6H_4CH_2NO_2$ exhibits nitroalkane anomaly, but not for p-$NO_2C_6H_4CH_2NO_2$, and that the transition state charge imbalance is an origin of anomaly.

INTRODUCTION

Proton transfer reactions of nitroalkanes are known to show abnormal reactivity, which is often called nitroalkane anomaly. The nitroalkane anomaly has been observed in several ways.[1−4] Pearson and Dillon reported in 1953 that a logarithmic plot of deprotonation rate constants of 26 different small carbon acids against corresponding equilibrium constants in water gave linear Brønsted plots with the slope of 0.56 and that the points of CH_3NO_2 and $CH_3CH_2NO_2$ deviated downward by 2 to 3 logarithmic units from the correlation line.[1] Thus, the proton-transfer rates for nitroalkanes are slower than expected from their acidities. Similar anomalous behavior of nitro-substituted compounds in proton-transfer and other reactions has been reported.[2] In a typical example, the pK_a value of RCH_2NO_2 decreases in the order $CH_3NO_2 > CH_3CH_2NO_2 > (CH_3)_2CHNO_2$ in water, whereas the rate of proton abstraction by hydroxide ion decreases in the same order. Here the reaction is slower for a more acidic substrate. An analogous system with an electron-withdrawing CN substituent, i.e., RR′CHCN, was reported to exhibit normal rate-equilibrium relationship in water.[5]

Another well-known example is shown in eq 1, in which the Brønsted α values are larger than unity, indicating that the substituent effect is larger on the rate than on the equilibrium. For example, the α value is 1.54 for R = H in H_2O,[3a,b] 1.37 for R = Me in 50% aqueous MeOH,[3c] and 1.18 for R = Me in 50% aqueous dioxane.[3d] Unusual behavior in the rate-equilibrium relationship of nitroalkanes has been reported not only for proton-transfer reactions but also for substitution reactions, in which nitronate anion acts as a nucleophile.[4]

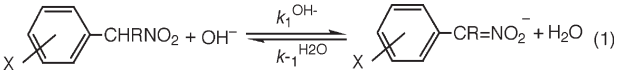

(1)

The origin of the anomaly has been interpreted in terms of different charge distribution at the transition state (TS) and the product state.[2,6] Chart 1 shows the resonance structure of nitronate anion. In the product anion, the negative charge is largely localized on the NO_2 group, whereas a partial negative charge developed within the $RCHNO_2$ moiety at the TS is in part on the CH_2 subgroup due to electrostatic interaction between the negatively charged carbon and the positively charged proton in-flight. Thus, a larger fraction of negative charge is localized on the carbon at the TS than at the product state, which explains the larger-than-unity Brønsted α values observed for reaction 1. At the same time, since the ability of resonatively stabilizing effect of the NO_2 group is not fully operating at the TS, the proton-transfer rates of RNO_2 are slower than expected from their pK_a's. The TS imbalance rationale has been developed by Bernasconi, for proton-transfer reactions of various substrates.[6] The TS imbalance can be conveniently detected by looking at the charge on C_α and on NO_2 both at the TS and the product anion, and such TS charge imbalance for nitroalkanes has indeed been confirmed computationally by several authors.[7−9]

Chart 1

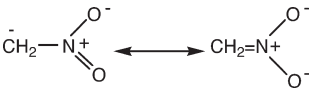

However, these molecular orbital (MO) calculations gave, at the same time, quite normal Brønsted α values, and thus no anomaly was detected in these gas-phase reactions.[8,9] Smaller α values, though still large, were observed for reaction 1 in non-hydroxylic solvents, which suggested important factors, such as

Received: February 21, 2011
Published: April 12, 2011

hydrogen-bond solvation, operating only in hydroxylic solvent.[10] These results implied that the TS charge imbalance might not be the sole origin of the nitroalkane anomaly.

Protonation of nitronate anion under acidic conditions has been shown experimentally to occur not on the carbon but on the oxygen site to give *aci*-nitro species (eq 2).[11−14] This apparently differs from the expectation for the protonation of nitronate anion with H_2O, which on the basis of the principle of microscopic reversibility has implicitly been assumed proceed via direct protonation to the carbon site of the anion to give nitro species and OH^-. Although it was assumed that *aci*-nitro species was on a blind alley and that the protonation with acid on nitronate led to nitro species via C-protonation, the reaction path via O-protonation and *aci*-nitro → nitro isomerization could not be eliminated on the basis of kinetics with a limited number of substrates. Recent theoretical calculations on the substituent effects on rate and equilibrium processes of important proton-transfer steps of $ArCH_2NO_2$ pointed out possible involvement of *aci*-nitro species in the main course of the reaction.[9]

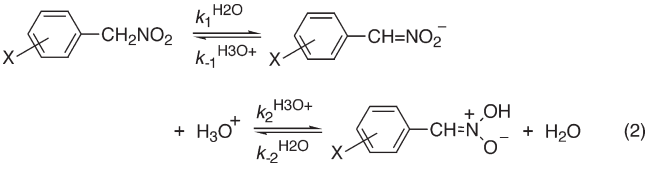

(2)

During preliminary kinetic study on the protonation of nitronate anion under acidic conditions, we found a possibility that *aci*-nitro species isomerizes to nitro species via bimolecular reaction with nitronate (eq 3). This process becomes competitive with direct C-protonation under the conditions that the protonation of nitronate anion is carried out with a deficient amount of acid. This finding prompted us to kinetically examine the whole processes involved in the proton-transfer reaction of phenylnitromethanes in order to understand the proton-transfer chemistry of nitroalkane. In particular, comparison was made between experimentally observed substituent effects with those derived computationally for each elementally step, which would allow us to understand the detailed processes of proton transfer of nitroalkane and the origin of the nitroalkane anomaly.

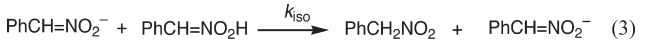

(3)

RESULTS AND DISCUSSION

Deprotonation with OH^-. We added some rate constant data to a large compilation of rates of base-promoted proton transfer of phenylnitroalkanes.[3] The rates of deprotonation of $XC_6H_4CH_2NO_2$ under pseudo-first-order conditions with NaOH in 300−600 molar excess at four different base concentrations were measured photometrically in 50% (v/v) aqueous MeOH at 25.0 °C by a stopped-flow method. Second-order rate constants are summarized in Table 1. The Hammett plot of the results in Figure 1 showed nice linear correlation for meta-points with a ρ value of 1.63 with the standard Hammett σ constants. The observed large positive ρ value is consistent with the nature of the reaction and qualitatively agrees with the value reported by Bordwell with a limited number of substituents (ρ = 1.28 for *m*-Me, H, *m*-Cl, and *m*-NO_2 in water, 26 °C).[3a] The difference of the ρ values is ascribed to the solvent effect, since it was reported that the ρ value for the deprotonation of $XC_6H_4CHCH_3NO_2$ was larger in 50% (v/v) aqueous MeOH (1.58) than in water (1.17).[3b] It is noticeable, however, that points of both strongly electron-withdrawing (*p*-NO_2) and electron-donating (*p*-MeO, *p*-Me) substituted derivatives deviated upward from the correlation line. Since the standard σ constants were apparently not appropriate for the anion-generating reaction, we examined linear free energy relation (LFER) against pK_a's of substituted phenols. The LFER plot in Figure 2 showed excellent correlation except for the *p*-NO_2 derivative, which deviated downward from the correlation. Thus, the resonance of *p*-NO_2 in the deprotonation TS is not as strong as that in the phenoxide ion. The observed considerable size of the slope (0.74) suggested that a significant amount of negative charge is developed at the benzylic carbon at the TS. The observed rate constants and the reported pK_a's of the four substituted phenylnitromethanes in 50% (v/v) aqueous MeOH[3b] gave the Brønsted α coefficient of 1.34, confirming the existence of anomaly in aqueous MeOH (Figure S1 in Supporting Information).

Protonation with H_2O. We have measured the rates of protonation on nitronate anions with water under neutral conditions, which corresponds to the reverse reaction of deprotonation with OH^-. This was planned because the pK_a values of $XC_6H_4CH_2NO_2$ were reported only for a limited number of derivatives and also because we had encountered difficulty in measuring pK_a's for additional derivatives. The rates of protonation could not be measured by a conventional way, since pK_a of $C_6H_5CH_2NO_2$ is much smaller than that of water and therefore

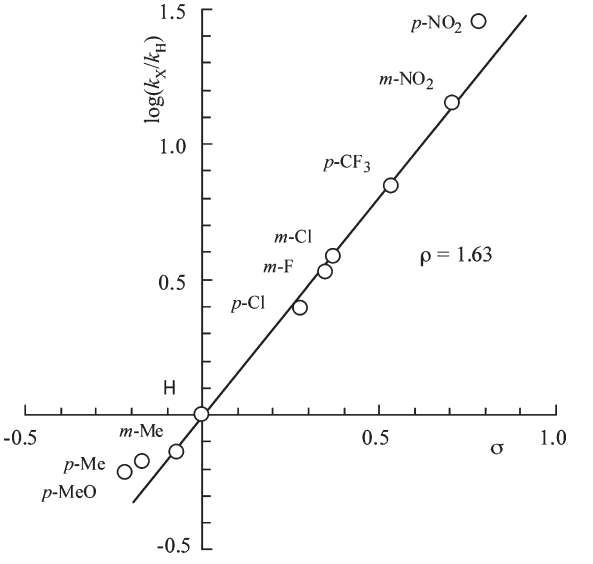

Figure 1. Hammett correlation of the deprotonation rate of $XC_6H_4CH_2NO_2$ with OH^- in 50% (v/v) aqueous MeOH at 25 °C.

Table 1. Second-Order Rate Constants for Deprotonation of $XC_6H_4CH_2NO_2$ with Hydroxide Ion in 50% (v/v) Aqueous MeOH at 25 °C

X	*p*-MeO	*p*-Me	*m*-Me	H	*p*-Cl	*m*-Cl	*m*-F	*p*-CF_3	*m*-NO_2	*p*-NO_2
k_2 (10^2 s^{-1} M^{-1})	2.08 ± 0.10	2.28 ± 0.07	2.46 ± 0.21	3.43 ± 0.18	8.48 ± 1.2	13.1 ± 1.2	11.4 ± 1.1	23.7 ± 2.4	48.4 ± 3.6	96.4 ± 3.4

dx.doi.org/10.1021/jo200383f |J. Org. Chem. 2011, 76, 3937–3945

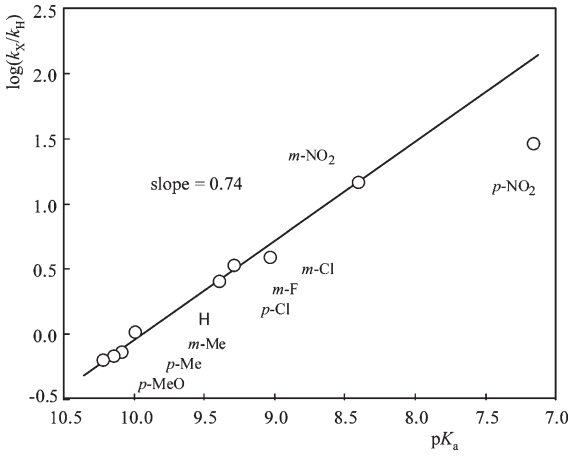

Figure 2. Correlation of the deprotonation rate of $XC_6H_4CH_2NO_2$ with OH^- in 50% (v/v) aqueous MeOH vs pK_a's of phenols.

the equilibrium is almost fully on the $PhCHNO_2^- + H_2O$ side. The rates were determined by running the reaction of nitronate anion in 50% D_2O/CD_3OD and following the uptake of deuterium in the anion by ^1H NMR (eq 4a).

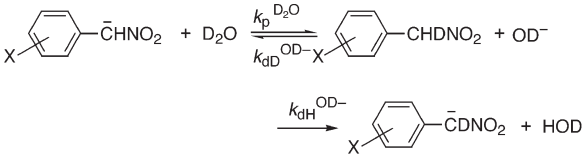

(4a)

$$k_{obs} = k_p^{D_2O} k_{dH}^{OD^-}/(k_{dD}^{OD^-} + k_{dH}^{OD^-})$$

$$k_p^{D_2O} = k_{obs}[1 + (k_{dD}^{OD^-}/k_{dH}^{OD^-})] \qquad (4b)$$

The pseudo-first-order rate constant (k_{obs}) is given by eq 4b. The second-order rate constant of deuterium uptake ($k_p^{D_2O}$) is obtained from the concentration of D_2O and isotope effect on deprotonation step ($k_{dH}^{OD^-}/k_{dD}^{OD^-}$). The second-order protonation rate constant ($k_p^{H_2O}$) can then be calculated, if the deuterium isotope effect ($k_p^{H_2O}/k_p^{D_2O}$) is known. We assigned 6.0 for both the combined primary and secondary deuterium isotope effects for deprotonation of $ArCHDNO_2$ ($k_{dH}^{OD^-}/k_{dD}^{OD^-}$) and the primary deuterium isotope effect for the protonation/deuteronation of $ArCH{=}NO_2^-$ with H_2O and D_2O ($k_p^{H_2O}/k_p^{D_2O}$), which are not bad estimates since k_H/k_D of 6.11 was reported for the deprotonation of $PhCL_2NO_2$ (L = H or D) with OH^- in water at 25 °C.[15] The pseudo-first-order rate constants, k_{obs}, for X = H determined at 40, 50, and 60 °C gave an excellent Eyring plot, from which the rate constant at 25 °C was calculated. For other substituted derivatives, rate constants at 25 °C were calculated from rate constants at 40 and 50 °C. The calculated protonation rate constants, $k_p^{H_2O}$, and the pseudo-first-order rate constants at 25 °C for nine substituted derivatives are listed, together with the activation parameters, in Table 2. Rate constants at higher temperatures are listed in Table S2. Note that these rate constants were obtained under the assumption that there is no deuteron transfer from CD_3OD and the deuterium isotope effects are the same (6.0) for all substituted derivatives. Although the calculated protonation rate constants may not be absolutely correct, they would be reliable in relative magnitude and should be useful in analyzing substituent effect. From the forward and reverse proton-transfer rate constants, the pK_a values of $XC_6H_4CH_2NO_2$ were calculated and are summarized in Table 2. Comparison of these pK_a's with those available in the literature shows that the pK_a's are reliable at least in their relative strength.

With a sufficient number of rate constants for the forward and reverse proton-transfer reactions of substituted phenylnitromethanes in a single solvent system, we now compare the substituent effects for both reactions. The substituent effects for the reverse reaction are illustrated in Figure 3. The observed positive ρ value of 0.45, calculated on the basis of meta substituents,

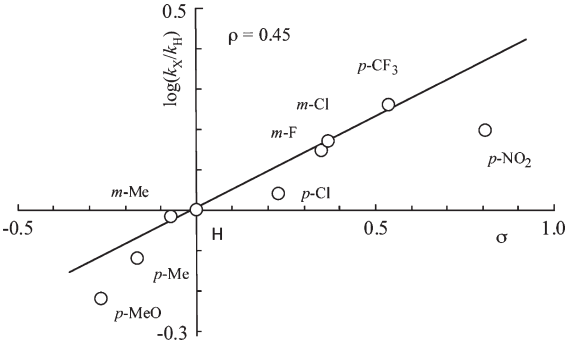

Figure 3. Hammett plot for the protonation of $XC_6H_4CH{=}NO_2^-$ with H_2O in 50% (v/v) aqueous MeOH at 25 °C.

Table 2. Activation Parameters, Pseudo-First-Order Rate Constants, and Second-Order Rate Constants for Protonation of $XC_6H_4CH{=}NO_2^-$ and pK_a Values of $XC_6H_4CH_2NO_2$ in 50% (v/v) MeOH at 25 °C

X	$\Delta H^{\ddagger}$ (kcal mol^{-1})	$\Delta S^{\ddagger}$ (cal K^{-1} mol^{-1})	k_{obs}[a] 1(10^{-6} s^{-1})	$k_p^{H_2O}$[b] (10^{-6} s^{-1} M^{-1})	pK_a[c]
p-MeO	22.5	−6.6	7.23 ± 0.08	1.82 ± 0.02	7.69
p-Me	21.6	−9.1	9.14 ± 0.14	2.30 ± 0.04	7.75
m-Me	21.7	−8.2	11.6 ± 0.10	2.90 ± 0.03	7.82 (8.00)
H	21.8	−7.7	12.1 ± 0.22	3.03 ± 0.05	7.69 (7.93)
p-Cl	21.8	−7.8	13.2 ± 0.07	3.31 ± 0.08	7.34
m-F	21.0	−9.9	16.8 ± 0.10	4.23 ± 0.02	7.31
m-Cl	21.0	−9.9	17.8 ± 0.30	4.48 ± 0.02	7.28 (7.48)
p-CF_3	20.6	−10.5	21.9 ± 0.17	5.49 ± 0.04	7.11
p-NO_2	19.7	−13.9	19.0 ± 0.29	4.76 ± 0.08	6.43 (6.49)

[a] Pseudo-first-order rate constant of deuterium uptake. [b] Second-order rate constant of protonation. [c] Calculated pK_a from forward and reverse rate constants. Numbers in parentheses are pK_a values reported in ref 3b.

dx.doi.org/10.1021/jo200383f |J. Org. Chem. 2011, 76, 3937–3945

Chart 2

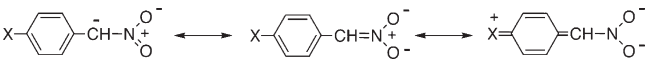

indicates that not only the forward but also the reverse reaction is accelerated by electron-withdrawing substituents, as expected for the reactions with nitroalkane anomaly.

Important and unexpected results in Figure 3, however, are the observed downward deviations for both electron-donating para substituents (*p*-MeO, *p*-Me, *p*-Cl) and the strongly electron-withdrawing para substituent (*p*-NO_2). The downward deviations for *p*-MeO, *p*-Me, and *p*-Cl can be rationalized by extra resonance stabilization in the nitronate anions by these substituents as illustrated in Chart 2. Thus, these para electron-donating substituents stabilize the anions and the protonation reactions become slower than expected from the meta correlation line. The downward deviation for *p*-NO_2 is striking. The TS imbalance rationale assumes that the amount of negative charge on the benzylic carbon would be larger at the proton-transfer TS than at the anion state, and hence the effect of substituents on the phenyl ring is larger at the TS. The TS imbalance operates since the benzylic NO_2 is a resonatively strong electron-withdrawing group, which accepts a large potion of negative charge in the anion leaving only partial charge on the benzylic carbon. The downward deviation for *p*-NO_2 in Figure 3 shows that the nitronate anion is strongly stabilized by the *p*-NO_2 substituent. It is implied that NO_2 on the phenyl ring competes with the benzylic NO_2 in delocalizing the negative charge and that a significant amount of negative charge resides on the $ArCH_2$ subgroup in the anion as in normal cases.

Protonation with H_3O^+ under Low Substrate Concentration. The rates of protonation on $XC_6H_4CH{=}NO_2^-$ under acidic conditions were measured photometrically in 50% (v/v) aqueous MeOH at 25 °C. The reaction was initiated by two ways; (1) nitronate anion was generated by the reaction of $XC_6H_4CH_2NO_2$ and NaOH, and then allowed to react with excess HCl, and (2) $XC_6H_4CH{=}NO_2Na$ prepared separately was treated with HCl.

With small excess of HCl over nitronate, the absorbance of the nitronate decreased without a change in λ_{max} (Figure 4A). By contrast, when large excess of HCl was added to a nitronate solution, the absorption maximum shifted within seconds from 294 nm (λ_{max} of the nitronate) to 277 nm, and then absorption of the spectrum decreases slowly (Figure 4B). The shift of the maximum is likely due to the formation of *aci*-nitro species. The rates of the reactions of $PhCH{=}NO_2^-$ (0.033 mM) with excess HCl were measured by following the absorbance at 277 nm. Reactions under pseudo-first-order conditions gave excellent linear first-order rate plots (Figure S2). However, reactions with lower acid concentrations did not show linear plots, and therefore the rate constants were calculated from the data of low fractions of reaction, and hence could be less reliable. The observed rate constants are listed in Table S2 and are plotted against the acid concentration in Figure 5. The apparent saturation kinetics indicates that the reaction proceeds either one of the two possible mechanisms. In one mechanism, the *aci*-nitro species is on the blind-alley, and phenylnitromethane is generated by C-protonation on the nitronate anion (eq 5). In the other mechanism, the nitro form is obtained through isomerization of the *aci*-nitro species (eq 6).

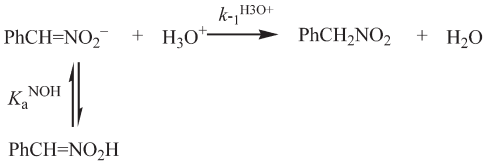

(5a)

$$k_{obs} = K_a^{NOH} k_{-1}^{H3O+} [H_3O^+]/(K_a^{NOH} + [H_3O^+]) \quad (5b)$$

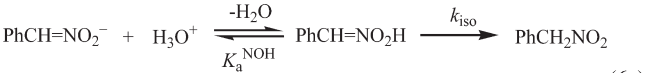

(6a)

$$k_{obs} = k_{iso} [H_3O^+]/(K_a^{NOH} + [H_3O^+]) \quad (6b)$$

Protonation on nitronate anions under acidic conditions has been investigated by several groups.[11−14,16−18] Bernasconi[11] and Terrier[12] have carried out kinetic study and successfully calculated $k_p^{H_3O+}$ and K_a^{NOH} for aliphatic and aromatic nitroalkanes under the assumption that the reaction proceeds by eq 5a.

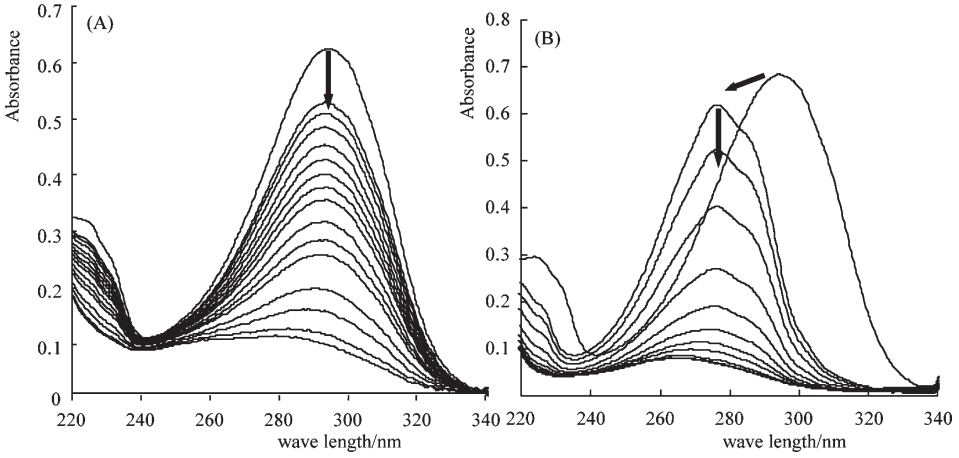

Figure 4. UV−vis absorption spectrum for protonation of nitronate anion in 50% (v/v) aqueous MeOH at 25 °C. (A) [$PhCH{=}NO_2^-$] = 0.033 mM, [HCl] = 0.033 mM, (B) [$PhCH{=}NO_2^-$] = 0.033 mM, [HCl] = 0.99 mM. Time intervals are 20 s at the initial part of the reaction and 60 min at the later part in both A and B.

dx.doi.org/10.1021/jo200383f |*J. Org. Chem.* 2011, 76, 3937–3945

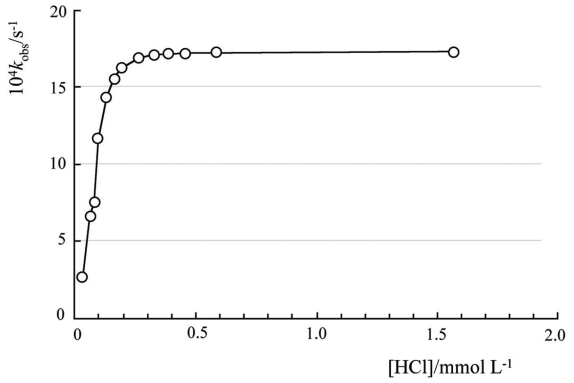

Figure 5. Observed rate constant variation with acid concentration for protonation of PhCH=NO_2^- (0.033 mM) in 50% (v/v) aqueous MeOH at 25 °C.

Table 3. Pseudo-First-Order Rate Constants for Protonation of $XC_6H_4CH{=}NO_2^-$ with H_3O^+ in 50% (v/v) Aqueous MeOH at 25 °C[a]

X	$10^4\ k_{obs}$ (s^{-1})
p-Me	9.07 ± 0.72
m-Me	15.0 ± 0.3
H	17.3 ± 0.7
p-Cl	32.8 ± 0.6
m-F	55.9 ± 1.0
m-Cl	64.9 ± 2.0
p-CF_3	116 ± 4

[a] [$XC_6H_4CH{=}NO_2^-$] = 0.033 mM.

Analysis of the present data with eq 5b gave pK_a^{NOH} and $k_{-1}^{H_3O+}$ as 4.2 and 34 $M^{-1}\ s^{-1}$, whereas analysis with eq 6b gave pK_a^{NOH} and k_{iso} as 4.2 and $2.1 \times 10^{-3}\ s^{-1}$, respectively. The calculated pK_a^{NOH} value is reasonable compared to the reported value (pK_a^{NOH} = 4.75 in 50% DMSO) at 20 °C. In principle, however, the two mechanisms are difficult to distinguish by the analysis of acid concentration dependence, since the rate is expressed in similar forms as shown in eqs 5b and 6b, respectively. In the present study, we examined the effect of substituent on the rate of protonation under high acid concentrations, where the rate is independent of the acid concentration and the substituent effect was compared with the calculated substituent effect (vide infra). Under such conditions, the rate constant, k_{obs}, would be $K_a^{NOH} k_{-1}^{H_3O+}$ and k_{iso} for mechanisms 5 and 6, respectively. The pseudo-first-order rate constants for protonation of $XC_6H_4CH{=}NO_2^-$ under acidic conditions are listed in Table 3 (and Table S3 in detail). The Hammett plot in Figure 6 gave a rather large ρ value of 1.49. It is much larger than the ρ value (0.45) for the protonation of $XC_6H_4CH{=}NO_2^-$ with neutral H_2O (Figure 3), which reflects that the mechanisms of protonation under neutral and acidic conditions are different; the protonation under basic conditions occurs on the nitronate anion, whereas the effective reactant species under high acidic concentrations is *aci*-nitro species.

Protonation with H_3O^+ under High Substrate Concentration. Since the absorption coefficients of nitronate anions were quite large, we have normally used a low substrate concentration (~0.03 mM) for the rate measurement. However, the use of such low concentrations required tedious procedures to eliminate atmospheric CO_2 in order to avoid an influence of CO_2 on the rate measurements. Thus, we also used a much higher substrate concentration (5.0 mM) and examined the effect of acid concentration on the reactivity. The rate constants determined with a batch method at 15 °C (see Supporting Information for details) are listed in Table S4 and illustrated in Figure 7.

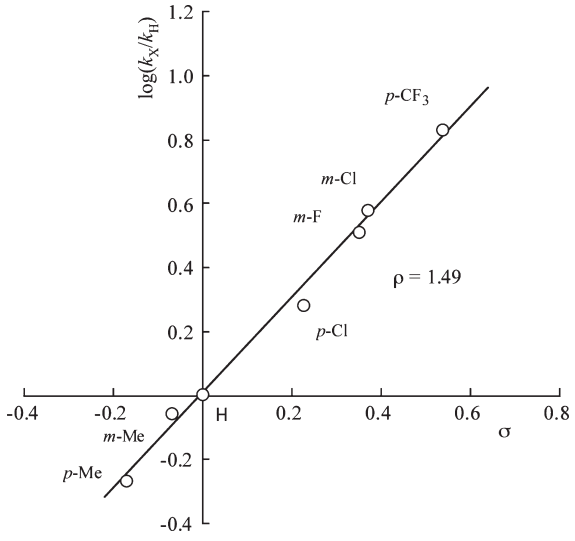

Figure 6. Hammett plot for protonation of $XC_6H_4CH{=}NO_2^-$ with H_3O^+ in 50% (v/v) aqueous MeOH at 25 °C.

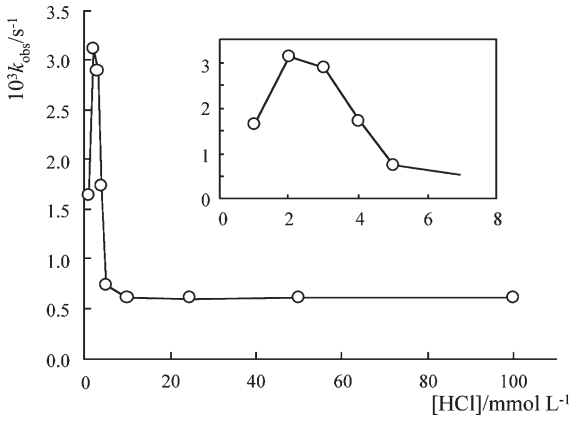

Figure 7. Observed rate constant variation with acid concentration for protonation of PhCH=NO_2^- (5.0 mM) in 50% (v/v) aqueous MeOH at 15 °C.

It was found that the protonation rates exhibited peculiar acid-concentration dependence as shown in Figure 7. Here, the rate constants at a high acid concentration region are constant at about $6.0 \times 10^{-4}\ s^{-1}$, which is in good agreement with the rate constant ($17.3 \times 10^{-4}\ s^{-1}$) determined at a lower substrate concentration (Figure 5) if the difference of reaction temperature is taken into account. At a low acid concentration region, however, the rate constants exhibit a sharp increase with a decrease of acid concentration, instead of showing saturation kinetics.

Since the reaction under low acid concentration conditions does not follow pseudo-first-order kinetics, the rates were determined only for the initial part of the reaction, and therefore the rate constants are less reliable. Nevertheless, the fact that the rate is faster at a lower acid concentration is clearly seen in the decay

dx.doi.org/10.1021/jo200383f |*J. Org. Chem.* 2011, 76, 3937–3945

Table 4. Hammett ρ Values for Various Proton-Transfer Steps of Substituted Phenylnitromethanes at 25 °C Calculated at B3LYP/6-31+G*

eq	reaction	ρ_{rate}	$\rho_{equilibrium}$
7	$XC_6H_4CH_2NO_2 + OH^-(H_2O)_2 \rightarrow XC_6H_4CH{=}NO_2^- + (H_2O)_3$	6.9[a]	12.6[a]
8	$XC_6H_4CH_2NO_2 + (H_2O)_2 \rightarrow XC_6H_4CH{=}NO_2H + (H_2O)_2$	2.3[a]	0.8[a]
9	$XC_6H_4CH{=}NO_2H + XC_6H_4CH{=}NO_2^- \rightarrow XC_6H_4CH{=}NO_2^- + XC_6H_4CH_2NO_2$	−2.2	−0.8
10	$XC_6H_4CH{=}NO_2^- + CH_2(NO_2)_2 \rightarrow XC_6H_4CH{=}NO_2H + CH(NO_2)_2^-$	−6.5	−12.1
11	$XC_6H_4CH{=}NO_2^- + CH_2(NO_2)_2 \rightarrow XC_6H_4CH_2NO_2 + CH(NO_2)_2^-$	−5.9	−13.0

[a] Data taken from ref 9.

plots in Figure S3 in Supporting Information. The fact suggested a possibility that the *aci*-nitro species initially formed by the O-protonation of nitronate anion reacts with the remaining nitronate anion to yield the nitronate and nitro species in a bimolecular reaction as shown in eq 3. This route becomes possible since the reaction of nitronate with a deficient amount of acid initially yields preferentially the O-protonated *aci*-nitro species, and under such circumstances the reaction of the *aci*-nitro and nitronate species to afford the nitro species is an endergonic process.

Since the initial protonation of nitronate occurs on O more rapidly than on C, if an effective *aci*-nitro−nitro transformation exists, then the protonation of nitronate to nitro may proceed through the *aci*-nitro route, especially when the protonation reaction is carried out at a higher substrate concentration than that (5 mM) in the protonation reaction here. A question then arises whether the *aci*-nitro route may be a significant route for deprotonation of nitroalkane with a base.

Comparison of Hammett ρ Values. Previous DFT calculations suggested on the basis of reaction energetics that the reaction of $ArCH{=}NO_2^-$ and H_2O proceeds via the direct C-protonation rather than the O-protonated *aci*-nitro intermediate ($ArCH{=}NO_2H$).[9] Although O-protonation is faster than C-protonation, the O-protonated state ($ArCH{=}NO_2H + OH^-$) is a minor component in the equilibrium with $ArCH{=}NO_2^- + H_2O$, and hence the route via *aci*-nitro species would be less favorable. However, it was also concluded that if there is an effective isomerization process whose barrier is much lower than $(H_2O)_2$-mediated isomerization (eq 8), $ArCH_2NO_2$ may be formed via the *aci*-nitro route. For the protonation of nitronate with acid, on the other hand, since the O-protonated state becomes a major component in the equilibrium, the energetic consideration suggested that the O-protonation−isomerization route could be well competitive with the direct C-protonation route, if a fast isomerization process is available.[9] With these arguments in mind, we have calculated ρ values for reactions 7−11, and compared the calculated ρ values with the ρ values determined experimentally in the present study.

Calculated ρ Values. The substituent effects on the rates and equilibria for reactions 7 and 8 in the gas phase have been calculated previously at the B3LYP/6-31+G* level of theory.[9] Reaction 8 is an isomerization of $XC_6H_4CH_2NO_2$ to $XC_6H_4CH{=}NO_2H$ through double proton transfer with $(H_2O)_2$ as a catalyst. The calculated ρ values were 6.9 (rate) and 12.6 (equilibrium) for reaction 7 and 2.3 (rate) and 0.8 (equilibrium) for reaction 8. In the present study, the substituent effects were calculated for reactions 9−11 at the same level of theory. Here, reaction 9 is an *aci*-nitro−nitro isomerization with the nitronate anion as a mediator, and reactions 10 and 11 are the O- and C-protonation on substituted nitronate anion by an acid. We used a carbon acid ($CH_2(NO_2)_2$) in reactions 10 and 11, since the use of H_3O^+ or HCl did not allow us to optimize TS structures.

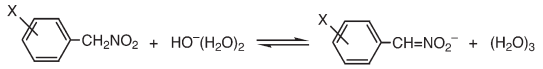

(7)

(8)

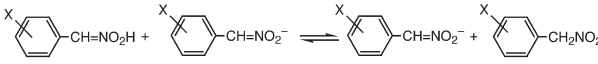

(9)

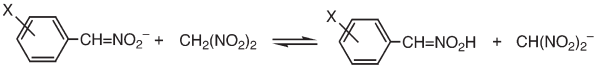

(10)

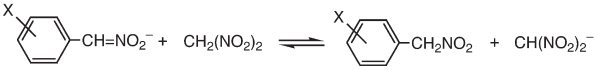

(11)

Hammett plots for the rates and equilibria for reactions 9−11 are illustrated in Figures S4−S6, and the calculated ρ values are summarized, together with the ρ values for reactions 7 and 8 in Table 4. The ρ value for the $ArCH_2NO_2 \rightarrow ArCH{=}NO_2^-$ equilibrium in the present study (13.0) is slightly different from that in reference[9] (12.6, eq 7), due to the difference in the number of substituents used in the calculations. It is interesting to note that the ρ_{rate} values for the deprotonation reactions with $OH^-(H_2O)_2$ (eq 7) and $CH(NO_2)_2^-$ (eq 11) are also similar (6.9 and 7.1 (= 13.0−5.9), despite the fact that the nature and the strength of these two bases are different.

Comparison of Calculated and Experimental ρ Values. The two mechanisms on the protonation of $XC_6H_4CH{=}NO_2^-$ with an acid (eqs 5 and 6) could be differentiated by comparing experimentally observed ρ values with the ρ values for elementary steps determined by the DFT calculations. If the protonation reaction proceeds via the *aci*-nitro route (eq 6), the experimental ρ value for each step could be assigned as shown in Scheme 1. Here, the ρ value (−1.20) for $XC_6H_4CH{=}NO_2^- \rightarrow XC_6H_4CH{=}NO_2H$ equilibrium was calculated from the pK_a^{NOH} values of two substrates (X = H and *p*-NO_2) in 50% DMSO,[11,12] and the ρ value (−1.22) was calculated from pK_a's of $XC_6H_4CH_2NO_2$. It is seen that the calculated ρ values for the nitronate → *aci*-nitro and the nitronate → nitro equilibria (−12.1 and −13.0) are much larger than the corresponding experimental values (−1.20 and −1.22) in both cases, likely due to the absence of solvation. In the O-protonation−isomerization mechanism, since $XC_6H_4CH{=}NO_2H$ is the effective reactant under acidic conditions,

dx.doi.org/10.1021/jo200383f |J. Org. Chem. 2011, 76, 3937–3945

Scheme 1

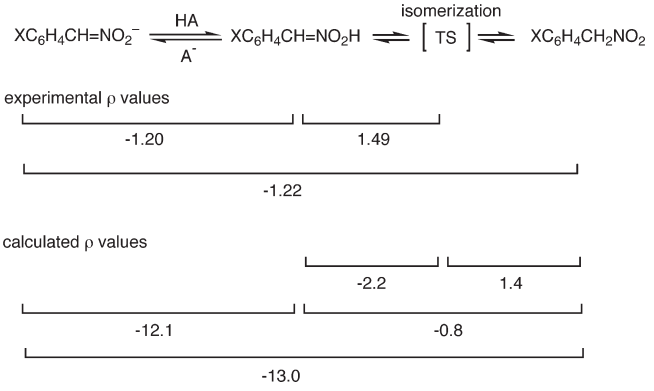

Scheme 2

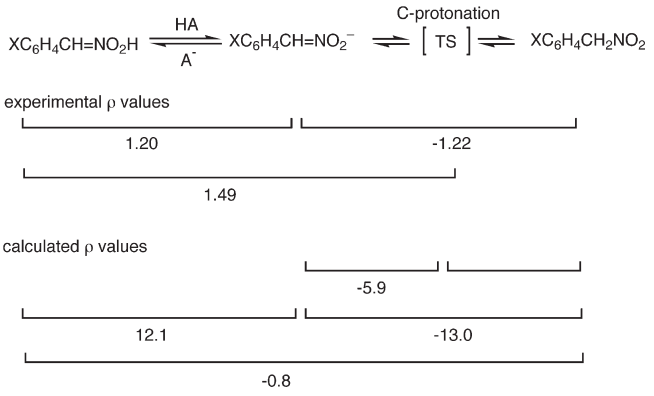

the experimental ρ value (1.49, Figure 6) is for the isomerization rate process for $XC_6H_4CH{=}NO_2H \rightarrow XC_6H_4CH_2NO_2$. The calculated ρ value for the same process in the gas phase is −2.2. These two values do not match, which clearly indicates that the reaction does not proceed through the O-protonation−isomerization mechanism in Scheme 1.

If, on the other hand, the direct C-protonation mechanism (eq 5) is assumed for the reaction, the ρ values are evaluated as shown in Scheme 2. In this mechanism, the substituent effect for the protonation $XC_6H_4CH{=}NO_2^-$ under acidic conditions would be the sum of the ρ value on the initial deprotonation equilibrium between $XC_6H_4CH{=}NO_2H$ and $XC_6H_4CH{=}NO_2^-$ and the ρ value for the C-protonation of $XC_6H_4CH{=}NO_2^-$, since the effective reactant is again $XC_6H_4CH{=}NO_2H$. The calculated overall ρ value for this route is 6.2 (12.1 + (−5.9)). Comparison of this ρ value and the experimental value (1.49) shows that the reaction mechanism illustrated in Scheme 2 is much more acceptable than the mechanism in Scheme 1. The difference of these two ρ values is well explained by the solvation effect. This, in turn, means that the deprotonation of $XC_6H_4CH_2NO_2$ with H_2O occurs via the direct deprotonation route rather than the *aci*-nitro route. The result further suggests that the protonation of $PhCH{=}NO_2^-$ with H_2O under neutral conditions proceeds through the direct C-protonation route, since the initial protonation equilibrium between $PhCH{=}NO_2^- + H_2O$ vs $PhCH{=}NO_2H + OH^-$ should almost completely on the nitronate side. In summary, the present kinetic study, together with previous[9] and present computational results showed that the *aci*-nitro species does not lie on the main course of the

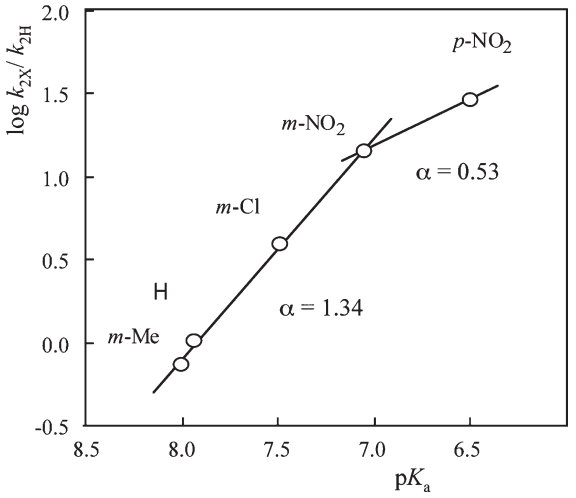

Figure 8. Brønsted correlation of the deprotonation rates of $XC_6H_4CH_2NO_2$ with hydroxide ion in 50% (v/v) aqueous MeOH at 25 °C. pK_a data was taken from refs 3a and 3b.

protonation reactions both under neutral and acidic conditions, or of the deprotonation reactions under basic and neutral conditions. This, in turn, means that the existence of *aci*-nitro species is not the origin of nitroalkane anomaly.

It is interesting to note that the Hammett plots reported in the literature for the deprotonation reaction of $XC_6H_4CH_2NO_2$ with OH^- did not include the data of the *p*-NO_2 derivative.[3a] The Brønsted slope α was calculated as the ratio of the two Hammett ρ values, on rate and equilibrium,[3b] and thus again the point of *p*-NO_2 was eliminated. We have now plotted the deprotonation rates determined in the present study against the pK_a reported in the literature in Figure 8. The Brønsted plot in Figure 8 clearly indicates that the point of *p*-NO_2 deviates downward from the correlation line. The slope gave the α value of 1.34 for all substituents except *p*-NO_2 and 0.53 for the line connecting *m*-NO_2 and *p*-NO_2. In Figure S7 is shown the Brønsted plot against the pK_a values determined in the present study (Table 2). Here also, the correlation gave nice straight line with an α value of larger than unity, but the point for the *p*-NO_2 derivative deviated downward. Thus, the so-called nitroalkane anomaly does not appear for the *p*-NO_2 substituted derivative. The two lines in Figure 8 implies that $XC_6H_4CH_2NO_2$ with a weakly electron-withdrawing or electron-donating X exhibit anomaly due to TS imbalance, reflecting small substituent effect on pK_a, whereas *p*-$NO_2C_6H_4CH_2NO_2$ does not show anomaly because the strongly electron-withdrawing *p*-$NO_2C_6H_4$ group can compete with the α-NO_2. It should be noted here that such TS imbalance is exalted by solvation to a level of showing nitroalkane anomaly due to an enhanced electron-withdrawing ability of NO_2 in protic solvents.[7,8,10]

CONCLUSION

The present extensive kinetic study for the proton-transfer reactions of phenylnitromethanes under various reaction conditions revealed that, although *aci*-nitro species may form during the proton-transfer reactions, it is not on the main reaction pathways. The Hammett plot for protonation of nitronate and a Brønsted plot including *p*-NO_2 showed that the nitroalkane anomaly exists for all substituted phenylnitromethanes except for the *p*-NO_2 derivative. The result is consistent with the notion that TS imbalance is the source of anomaly.

dx.doi.org/10.1021/jo200383f |*J. Org. Chem.* 2011, 76, 3937–3945

EXPERIMENTAL SECTION

Materials. Water (liquid chromatography grade) was fractionally distilled and degassed before use and mixed with fractionally distilled methanol (liquid chromatography grade) to make 50% (v/v) aqueous methanol. D_2O (Merck, 99.9%) and methanol-d_4 (ACROS, 99.8%) were used as received.

Substituted phenylnitromethanes were prepared from substituted phenylacetonitriles,[19] from phenylacetic acid or from benzyl bromide. Substituted phenylnitromethanes were purified by either column chromatography (H, *m*-Me, *p*-Me, *p*-MeO, *m*-F, *m*-Cl, *p*-Cl, and *p*-CF_3 derivatives) or recrystallization (*m*-NO_2 and p-NO_2) or both (*p*-CF_3). Sodium salts of phenylnitromethanes were prepared by running the reaction of phenylnitromethanes with sodium in anhydrous EOH/Et_2O mixed solvent.

Preparation of Phenylnitromethanes from Phenylacetonitriles. *$C_6H_5CH_2NO_2$.* To Na metal (6.10 g, 0.265 mol) dissolved in ice-cooled anhydrous EtOH (75 mL) was added dropwise a mixture of $PhCH_2CN$ (29.5 g, 0.252 mol) and $MeONO_2$ (70.0 g, 0.909 mol) under stirring at such a rate that the solution temperature stayed at 4−8 °C. The stirring was continued for 3 h, and the solution was stored in refrigerator overnight. The precipitate was collected by filtration and washed with anhydrous Et_2O. The filtrate was condensed by rotary evaporator, and the resultant precipitate was filtered and washed with anhydrous Et_2O. The precipitate was combined with the first lot and dried over silica gel. The combined precipitate was boiled with NaOH (41.6 g, 1.04 mol) in H_2O (160 mL) for 3 h, allowed to cool to room temperature, and was added to 10 g of ice. The reaction mixture was cooled at −20 to −10 °C and acidified with conc HCl. The solution was extracted with Et_2O, and the organic layer was washed with aqueous $NaHCO_2$ and water and dried over $MgSO_4$. Yield, 48.8%. ^{1}H NMR ($CDCl_3$, 400 MHz): δ 7.41−7.46 (m, 5H), 5.44 (s, 2H). ^{1}H NMR (CD_3OD, 400 MHz): δ 7.42−7.49 (m, 5H), 5.57 (s, 2H). ^{13}C NMR (CD_3OD, 400 MHz): δ 132.2, 131.2, 130.7, 130.0, 80.6.

p-$MeC_6H_4CH_2NO_2$. Yield, 28.9%. ^{1}H NMR ($CDCl_3$, 400 MHz): δ 7.34 (d, J = 7.8 Hz, 2H), 7.23 (d, J = 7.8 Hz, 2H), 5.40 (s, 2H), 2.38 (s, 3H).

m-$MeC_6H_4CH_2NO_2$. Yield: 45.5%. ^{1}H NMR ($CDCl_3$, 400 MHz): δ 7.24−7.34 (m, 4H), 5.40 (s, 2H), 2.38 (s, 3H). ^{1}H NMR (CD_3OD, 400 MHz): δ 7.26−7.32 (m, 4H), 5.52 (s, 2H), 2.36 (s, 3H). ^{13}C NMR (CD_3OD, 400 MHz): δ 140.0, 132.1, 131.7, 131.4, 129.8, 128.2, 80.7, 21.3.

m-$FC_6H_4CH_2NO_2$. Yield: 71.1%. ^{1}H NMR ($CDCl_3$, 400 MHz): δ 7.42 (td, J = 7.8, 5.8 Hz, 1H), 7.24 (d, J = 7.8 Hz, 1H), 7.14−7.21 (m, 2H), 5.44 (s, 2H).

p-$ClC_6H_4CH_2NO_2$. Yield: 40.7%. ^{1}H NMR ($CDCl_3$, 400 MHz): δ 7.39−7.43 (m, 4H), 5.41 (s, 2H).

p-$CF_3C_6H_4CH_2NO_2$. Yield: 71.4%. Mp 41−42 °C. ^{1}H NMR ($CDCl_3$, 400 MHz): δ 7.72 (d, J = 8.2 Hz, 2H), 7.60 (d, J = 8.2 Hz, 2H), 5.51 (s, 2H).

Preparation of Phenylnitromethanes from Phenylacetic Acids. *p-$MeOC_6H_4CH_2NO_2$.* To diisopropylamine (12.5 g, 123 mmol) in 100 mL of anhydrous THF cooled with a dry ice/EtOH bath were added under N_2 atmosphere *n*-BuLi (2.6 M, 15.2 mL, 117 mmol) and HMPA (9.15 g, 51.0 mmol) in 40 mL of anhydrous THF by using a hypodermic syringe, and the solution was allowed to warm up to 0 °C. An anhydrous THF (40 mL) solution of *p*-$MeOC_6H_4CH_2CO_2H$ (8.48 g, 51.0 mmol) was added dropwise to the LDA solution at 0 °C, and the solution was stirred at room temperature for 1.5 h. The solution was cooled again with a dry ice/EtOH bath, and $MeONO_2$ (11.4 g, 153 mmol) was added and kept stirring for 1 h at the same temperature. After addition of CH_3CO_2H (7 mL), the reaction solution was warmed up to 0 °C, HCl (4 M, 60 mL) was added, and the mixture was extracted with ether. Yield: 81.6%. ^{1}H NMR ($CDCl_3$, 400 MHz): δ 7.38 (d, J = 8.7 Hz, 2H), 6.94 (d, J = 8.7 Hz, 2H), 5.37 (s, 2H), 3.83 (s, 3H).

Preparation of Phenylnitromethanes from Benzyl Bromides. *m-$NO_2C_6H_4CH_2NO_2$.* In 500 mL flask were placed $AgNO_2$ (5.26 g, 34.1 mmol) and Et_2O (240 mL), and the flask was purged by N_2 and covered by aluminum foil. At room temperature, *m*-$NO_2C_6H_4CH_2Br$ (6.70 g, 31.1 mmol) in Et_2O (150 mL) was added by using a hypodermic syreinge. The reaction solution was stirred for 22 h at room temperature, filtered, washed with H_2O, and dried over $MgSO_4$. Yield: 77.4%. Mp 94−95 °C. ^{1}H NMR ($CDCl_3$, 400 MHz): δ 8.34−8.36 (m, 2H), 7.82 (d, J = 7.8 Hz, 1H), 7.67 (t, J = 7.8 Hz, 1H), 5.56 (s, 2H). ^{1}H NMR (CD_3OD, 400 MHz): δ 8.42 (s, 1H),.8.34 (d, J = 8.0 Hz, 1H), 7.91 (d, J = 8.0 Hz, 1H), 7.71 (t, J = 8.0 Hz, 1H), 5.77 (s, 2H). ^{13}C NMR (CD_3OD, 400 MHz): δ 144.0, 137.7, 133.8, 131.3, 126.5, 126.4, 78.9.

m-$ClC_6H_4CH_2NO_2$. Yield: 81.3%. ^{1}H NMR ($CDCl_3$, 400 MHz): δ 7.33−7.47 (m, 2H), 5.41 (s, 2H). ^{1}H NMR (CD_3OD, 400 MHz): δ 7.53 (s, 1H),.7.39−7.48 (m, 3H), 5.59 (s, 2H). ^{13}C NMR (CD_3OD, 400 MHz): δ 135.6, 134.0, 131.5, 131.4, 130.8, 129.7, 79.6.

p-$NO_2C_6H_4CH_2NO_2$. Yield: 50.7%. Mp 90−91 °C. ^{1}H NMR ($CDCl_3$, 400 MHz): δ 8.32 (d, J = 8.7 Hz, 2H), 7.67 (d, J = 8.7 Hz, 2H), 5.56 (s, 2H). ^{1}H NMR (CD_3OD, 400 MHz): δ 8.30 (d, J = 8.7 Hz, 2H),.7.75 (d, J = 8.7 Hz, 2H), 5.77 (s, 2H). ^{13}C NMR (CD_3OD, 400 MHz): δ 150.1, 138.5, 132.7, 124.9, 79.1.

Preparation of Sodium Salt of Phenylnitromethanes. *$C_6H_5CH{=}NO_2Na$.* To a 50% (v/v) mixture of anhydrous EtOH and anhydrous Et_2O (10.8 mL) was added Na (0.460 g, 20.0 mmol), and the mixture was stirred until Na was completely dissolved. To this mixture, anhydrous Et_2O (54 mL) was added, and then $PhCH_2NO_2$ (3.01 g, 22.0 mmol) in anhydrous Et_2O (13.2 mL) was added dropwise. The resultant precipitate was collected and washed with anhydrous Et_2O and dried. Yield: 95.8%. ^{1}H NMR (CD_3OD, 400 MHz): δ 7.87 (d, J = 7.8 Hz, 2H), 7.29 (t, J = 7.8 Hz, 2H), 7.16 (t, J = 7.8 Hz, 1H), 6.98 (s, 1H). ^{13}C NMR (CD_3OD, 400 MHz): δ 134.4, 129.1, 127.6, 127.5, 116.9.

p-$MeOC_6H_4CH{=}NO_2Na$. Yield: 57.6%. ^{1}H NMR (CD_3OD, 400 MHz): δ 7.83 (d, J = 9.2 Hz, 2H), 6.92 (s, 1H), 6.88 (d, J = 9.2 Hz, 2H), 3.79 (s, 3H).

p-$MeC_6H_4CH{=}NO_2Na$. Yield: 74.5%. ^{1}H NMR (CD_3OD, 400 MHz): δ 7.75 (d, J = 8.0 Hz, 2H), 7.12 (d, J = 8.0 Hz, 2H), 6.94 (s, 1H, CH), 2.30 (s, 3H).

m-$MeC_6H_4CH{=}NO_2Na$. Yield: 74.8%. ^{1}H NMR (CD_3OD, 400 MHz): δ 7.72 (s, 1H), 7.64 (d, J = 7.8 Hz, 1H), 7.17 (t, J = 7.8 Hz, 1H), 6.99 (d, J = 7.8 Hz, 1H), 6.94 (s, 1H), 2.32 (s, 3H). ^{13}C NMR (CD_3OD, 400 MHz): δ 138.7, 134.2, 129.1, 128.5, 128.6, 124.9, 117.2, 21.6.

m-$FC_6H_4CH{=}NO_2Na$. Yield: 60.2%. ^{1}H NMR (CD_3OD, 400 MHz): δ 7.93 (d, J_{HF} = 12.0 Hz, 1H), 7.38 (d, J = 8.0 Hz, 1H), 7.26 (td, J = 8.0, J_{HF} = 5.6 Hz, 1H), 6.98 (s, 1H), 6.86 (dd, J = 8.0, J_{HF} = 8.0 Hz, 1H).

p-$ClC_6H_4CH{=}NO_2Na$. Yield: 70.3%. ^{1}H NMR (CD_3OD, 400 MHz): δ 7.86 (d, J = 9.2 Hz, 2H), 7.27 (d, J = 9.2 Hz, 2H), 6.96 (s, 1H).

m-$ClC_6H_4CH{=}NO_2Na$. Yield: 74.2%. ^{1}H NMR (CD_3OD, 400 MHz): δ 8.14 (s, 1H), 7.57 (d, J = 7.8 Hz, 1H), 7.25 (t, J = 7.8 Hz, 1H), 7.13 (d, J = 7.8 Hz, 1H), 6.95 (s, 1H). ^{13}C NMR (CD_3OD, 400 MHz): δ 136.6, 135.2, 130.4, 127.0, 126.7, 125.6, 115.3.

p-$CF_3C_6H_4CH{=}NO_2Na$. Yield: 62.8%. ^{1}H NMR (CD_3OD, 400 MHz): δ 8.03 (d, J = 8.2 Hz, 2H), 7.55 (d, J = 8.2 Hz, 2H), 7.04 (s, 1H).

m-$NO_2C_6H_4CH{=}NO_2Na$. Yield: 60.9%. ^{1}H NMR (CD_3OD, 400 MHz): δ 9.03 (s, 1H), 8.01 (d, J = 7.8 Hz, 1H), 7.97 (d, J = 7.8 Hz, 1H), 7.49 (t, J = 7.8 Hz, 1H), 7.09 (s, 1H). ^{13}C NMR (CD_3OD, 400 MHz): δ 149.9, 136.8, 132.6, 132.6, 130.1, 121.1, 114.3.

p-$NO_2C_6H_4CH{=}NO_2Na$. Yield: 74.4%. ^{1}H NMR (CD_3OD, 400 MHz): δ 8.14 (d, J = 9.2 Hz, 2H), 8.03 (d, J = 9.2 Hz, 2H), 7.08 (s, 1H). ^{13}C NMR (CD_3OD, 400 MHz): δ 145.8, 141.9, 126.7, 124.6. 114.6.

Rate Measurements. *Measurement of Deprotonation Rates.* Rate constants for the deprotonation of $XC_6H_4CH_2NO_2$ with OH^- in aqueous 50% (v/v) MeOH at 25 ± 0.1 °C were determined by

dx.doi.org/10.1021/jo200383f |*J. Org. Chem.* 2011, 76, 3937–3945

following the decay of absorbance of $XC_6H_4CH_2NO_2$ at 297.0 nm for X = *p*-MeO (295.8 nm, *p*-Me; 294.5 nm, *m*-Me; 295.6 nm, H; 303.3 nm, *p*-Cl; 299.5 nm, *m*-Cl; 301.2 nm, *m*-F; 311.4, *p*-CF_3; 304 nm, *m*-NO_2; 391.0 nm, *p*-NO_2) with a stopped-flow instrument. The initial concentration of $XC_6H_4CH_2NO_2$ was 0.050 mM, and that of OH^- was 1.5, 2.0, 2.5, or 3.0 mM.

Measurement of the Rates of Protonation of Nitronate Anion (H-D Exchange). Protonation reaction was initiated by mixing $C_6H_5CH{=}NO_2$-Na (79.6 mg, 0.500 mmol) and DMSO (internal standard, 20 mg, 0.25 mmol) in D_2O (1.0 mL) and CD_3OD (1.0 mmol) at a desired temperature (t = 0). At preset intervals, 0.1 mL of the reaction solution was transferred with a hypodermic syringe to an NMR tube, which contains 0.4 mL of D_2O, and cooled down to freeze in a low-temperature bath (←20 °C). The protonation reaction was practically stopped when the solution was mixed with a large potion of D_2O, since the protonation is very slow in aqueous MeOH with a high H_2O content. The proton NMR spectra were then recorded, and the relative intensity of the benzylic proton (δ = 7.08) with respect to CH_3 signal of DMSO was used to follow the reaction.

Measurement of the Rates of Protonation of Nitronate Anion (Low Acid Concentration). Rate constants for the protonation of $C_6H_5CH{=}NO_2Na$ with HCl in aqueous 50% (v/v) MeOH at 25 ± 0.1 °C were determined by following the decay of absorbance of the equilibrium mixture of $XC_6H_4CH{=}NO_2Na$ and $XC_6H_4CH{=}NO_2H$ at 276.0−294.0 nm photometrically. The initial concentration of $XC_6H_4CH{=}NO_2Na$ was 0.033 mM. The rate constants for $C_6H_5CH{=}NO_2Na$ with different acid concentrations are listed in Table S3. Rate constants for $XC_6H_4CH{=}NO_2Na$ are summarized in Table S4. Typical rate plots are illustrated in Figure S2.

Measurement of the Rates of Protonation of $PhCH{=}NO_2^-$ (High Substrate Concentration). The reactions at higher substrate concentrations were carried out in a flask with the concentration of $XC_6HCH{=}NO_2Na$ of 5 mM at 15 ± 0.1 °C. The rate constants were determined by a batch method, in which 0.1 mL of the reaction solution was taken out at preset intervals, diluted in a 10 mL volumetric flask, and subjected to UV measurement. The results are listed in Table S4. Examples of rate plots are shown in Figure S3.

Calculations. Separated reactants, TSs, and products for reactions 9−11 were calculated at the B3LYP/6-31+G* level of theory.[20] Full frequency analyses were carried out to confirm that the optimized structures were minima or saddle points on the potential energy surface. All activation and reaction energies reported are relative to separated reactants in kcal mol^{-1}. We use enthalpies rather than free energies, since calculated entropies, and hence free energies as well, are known to be less reliable and not suitable for linear free energy analyses. Hammett plots were made by using relative activation or reaction enthalpies at 298 K.

■ ASSOCIATED CONTENT

Supporting Information. Kinetic data, Hammett and Brønsted plots, and computational results. This material is available free of charge via the Internet at http://pubs.acs.org.

■ AUTHOR INFORMATION

Corresponding Author
*E-mail: yamataka@rikkyo.ac.jp.

■ ACKNOWLEDGMENT

The study was in part supported by the Grant-in-Aid for Scientific Research from the Ministry of Education, Culture, Sports, Science and Technology, Japan.

■ REFERENCES

(1) Pearson, R. G.; Dillon, R. L. *J. Am. Chem. Soc.* **1953**, *75*, 2439.
(2) Kresge, A. J. *Can. J. Chem.* **1974**, *52*, 1897. Kresge, A. J.; Drake, D. A.; Chang, Y. *Can. J. Chem.* **1974**, *52*, 1889.
(3) (a) Bordwell, F. G.; Boyle, W. J., Jr. *J. Am. Chem. Soc.* **1971**, *93*, 511. (b) Bordwell, F. G.; Boyle, W. J., Jr. *J. Am. Chem. Soc.* **1972**, *94*, 3907. (c) Bordwell, F. G.; Boyle, W. J., Jr; Yee, K. C. *J. Am. Chem. Soc.* **1970**, *92*, 5926. (d) M. Fukuyama, M.; Flanagan, P. W. K.; Williams, F. T., Jr.; Frainier, L.; Miller, S. A.; Shechter, H. *J. Am. Chem. Soc.* **1970**, *92*, 4689.
(4) Grinblat, J.; Ben-Zion, M.; Hoz, S. *J. Am. Chem. Soc.* **2001**, *123*, 10738. Eliad, L.; Hoz, S. *J. Phys. Org. Chem.* **2002**, *15*, 540. Bug, T.; lewek, T.; Mayr, H. *J. Org. Chem.* **2004**, *69*, 7565.
(5) Richard, J. P.; Williams, G.; Gao, J. *J. Am. Chem. Soc.* **1999**, *121*, 715.
(6) Bernasconi, C. F. *Acc. Chem. Res.* **1987**, *20*, 301. Bernasconi, C. F. *Acc. Chem. Res.* **1992**, *25*, 9. Bernasconi, C. F. *Adv. Phys. Org. Chem.* **1992**, *27*, 116. Bernasconi, C. F.; Wenzel, P. J. *J. Am. Chem. Soc.* **1994**, *116*, 5405. Bernasconi, C. F.; Wenzel, P. J. *J. Am. Chem. Soc.* **1996**, *118*, 11446. Bernasconi, C. F. *Adv. Phys. Org. Chem.* **2010**, *44*, 223.
(7) (a) Bernasconi, C. F.; Wenzel, P. J.; Keeffe, J. R.; Gronert, S. *J. Am. Chem. Soc.* **1997**, *119*, 4008. (b) Bernasconi, C. F.; Wenzel, P. J. *J. Am. Chem. Soc.* **2001**, *123*, 2430.
(8) Yamataka, H.; Mustanir; Mishima, M. *J. Am. Chem. Soc.* **1999**, *121*, 10223.
(9) Sato, M.; Kitamura, Y.; Yoshimura, N.; Yamataka, H. *J. Org. Chem.* **2009**, *74*, 1267.
(10) Keeffe, J. R.; Morey, J.; Palmer, C. A.; Lee, J. C. *J. Am. Chem. Soc.* **1979**, *101*, 1295.
(11) Bernasconi, C. F.; Kliner, D. A. V.; Mullin, A. S.; Ni, J. X. *J. Org. Chem.* **1988**, *53*, 3342.
(12) Moutiers, G.; Thuet, V.; Terrier, F. *J. Chem. Soc., Perkin Trans. 2* **1997**, 1479.
(13) Turnbull, D.; Maron, S. H. *J. Am. Chem. Soc.* **1943**, *65*, 212.
(14) Maron, S. H.; La Mer, V. K. *J. Am. Chem. Soc.* **1939**, *61*, 692.
(15) Bordwell, F. G.; Boyle, W. J., Jr. *J. Am. Chem. Soc.* **1975**, *97*, 3447.
(16) Sun, S. F.; Folliard, J. T. *Tetrahedron* **1971**, *27*, 323.
(17) Pearson, R. G.; Dillon, R. L. *J. Am. Chem. Soc.* **1950**, *72*, 3574.
(18) Edward, J. T.; Tremaine, P. H. *Can. J. Chem.* **1971**, *49*, 3483.
(19) *Organic Synthesis*; Wiley: New York, 1943; p 512.
(20) Frisch, M. J. et al. *Gaussian 03, Revision C.02*; Gaussian, Inc.: Wallingford, CT, 2004.